

RESEARCH PAPER

## Effect of Annealing Temperature on Structural, Electrical and Optical Properties of TiO<sub>2</sub> Nanopowder

Shubhra Mathur<sup>1\*</sup>, Mamta Arya<sup>1</sup>, Rohit Jain<sup>1</sup>, Suman Kumar Sharma<sup>2</sup>

<sup>1</sup> Department of Physics, Jagannath Gupta Institute of Engineering & Technology, Sitapura Industrial Area, Jaipur, 302022, India

<sup>2</sup> Department of Physics, Malaviya National Institute of Technology, JLN Marg, Jaipur, 302017, India

### ARTICLE INFO

#### Article History:

Received 08 February 2017

Accepted 14 March 2017

Published 01 April 2017

#### Keywords:

Annealing

Band gap

Titanium

X-ray diffraction

### ABSTRACT

TiO<sub>2</sub> nanopowder is prepared by simple sol-gel method using starting material as titanium isopropoxide with methanol and annealed at 600°C, 700°C and 800°C for 1 hour in air. X-ray diffraction pattern revealed the presence of both anatase and rutile phase in TiO<sub>2</sub> specimens annealed at different temperatures. It is observed that the content of rutile phase and crystallite size increases with increase in annealing temperature. Scanning electron microscopy (SEM) is used to study surface morphology of TiO<sub>2</sub> specimens annealed at different temperatures. Using Tauc plot it is observed that energy band gap decreases with increase in annealing temperature. I-V curve of TiO<sub>2</sub> specimen shows that current increases with increase in annealing temperature. The preparation method is optimized by changing the concentration of titanium isopropoxide which leads to mixed phase (anatase and rutile) TiO<sub>2</sub> nanopowder with a lower energy band gap value which may play an important role in gas sensing applications.

### How to cite this article

Mathur S, Arya M, Jain R, Sharma S. K. Effect of Annealing Temperature on Structural, Electrical and Optical Properties of TiO<sub>2</sub> Nanopowder. J Nanostruct, 2017; 7(2):121-126. DOI: 10.22052/jns.2017.02.005

### INTRODUCTION

Titanium dioxide (TiO<sub>2</sub>) is considered as one of the important semiconductor metal oxide due to its wide range of applications such as in solar cells, self cleaning surfaces, CO<sub>2</sub> reduction and gas sensing [1-3]. TiO<sub>2</sub> exists in three polymorphs anatase, rutile and brookite. Rutile is the most stable phase whereas anatase and brookite are metastable phases. Anatase and brookite can transform to rutile phase on heating. The energy band gap for anatase and rutile phases are 3.2 eV and 3.0 eV respectively [4].

In recent years mixed phase (anatase and rutile) nanostructured TiO<sub>2</sub> was found to exhibit improved gas sensing properties [5, 6]. Therefore it is desirable to prepare mixed phase TiO<sub>2</sub> nanopowder by a simple sol-gel method. In our investigation the preparation method of mixed

phase TiO<sub>2</sub> nanopowder is optimized by changing the concentration of titanium isopropoxide which acts as a starting material. The prepared TiO<sub>2</sub> nanopowder shows lower band gap value as compared to data reported in the literature [6, 7]. The lower band gap value and the presence of mixed phase (anatase and rutile) in TiO<sub>2</sub> nanopowder may lead to improved gas sensing properties [5-8]. Hence it will be beneficial to understand the effect of annealing temperature on its structural, electrical and optical properties.

### MATERIALS AND METHODS

Titanium isopropoxide (TTIP) and methanol are used as starting materials. The chemicals used are of analytical research grade. 3.5 ml of titanium isopropoxide (TTIP) is added in 40 ml methanol. This results in a milky white solution. Magnetic

\* Corresponding Author Email: [shubhramathur3@gmail.com](mailto:shubhramathur3@gmail.com)

stirrer is used to stir the solution vigorously for 1:30 hrs. at a temperature  $57 \pm 3^\circ\text{C}$ . The gel thus produced is kept for 12 hrs. at room temperature. Therefore powder is obtained and annealed at temperatures  $600^\circ\text{C}$ ,  $700^\circ\text{C}$  and  $800^\circ\text{C}$  for 1 hour in air [6]. X-ray diffraction pattern (XRD) of TiO<sub>2</sub> specimens annealed at different temperatures is recorded using CuK $\alpha$  radiation. The UV-absorption spectra are recorded on Shimadzu-1800 UV- spectrophotometer by dispersing TiO<sub>2</sub> nanopowder in deionized water. In order to study electrical properties pellets having diameter 10 mm of TiO<sub>2</sub> nanopowder specimens are formed by Hydraulic pellet press and copper wire with a silver paste is used to form metal contacts on specimens. Kiethley-2400 source meter with two probe set up is used to record I-V characteristics at room temperature.

## RESULTS AND DISCUSSION

X-ray diffraction peaks show the presence of both anatase and rutile phases in various TiO<sub>2</sub> specimens as shown in Fig 1. The diffraction angles are in good agreement with JCPDS no 21-1272 for anatase, JCPDS no 21-1276 for rutile and data reported in the literature [1, 9]. The average crystallite size for various TiO<sub>2</sub> specimens annealed at  $600^\circ\text{C}$ ,  $700^\circ\text{C}$  and  $800^\circ\text{C}$  is calculated using Scherrer's formula [9].

$$D = 0.89\lambda / \beta \cos\theta \quad (1)$$

where D is crystallite size in nanometer,  $\beta$  is the full width at half maximum (FWHM) in radian,  $\lambda$  is the wavelength of the X-ray which is 0.15406 nm for Cu target K $\alpha$  radiation and  $\theta$  is the Bragg angle. The content of anatase and rutile phase is calculated using formula [1]:

$$X_a = 1 / 1 + 1.26 (I_r / I_a) \quad (2)$$

where  $X_a$  is the weight fraction of anatase in the mixture,  $I_a$  and  $I_r$  are intensities of anatase (101) and rutile (110) diffraction peaks. The average crystallite size and content of anatase and rutile phase for TiO<sub>2</sub> specimens annealed at different temperatures are summarized in Table 1. It is observed (see Table 1) that the content of rutile phase and an average crystallite size increases with increase in annealing temperature. Moreover, it was reported that the presence of mixed anatase and rutile phase leads to improved gas sensing properties [5, 6]. This shows that the change in content of anatase and rutile phase present in TiO<sub>2</sub> nanopowder after annealing may lead to interesting gas sensing properties. It is noteworthy here that the formation of rutile phase at an annealing temperature of  $800^\circ\text{C}$  was reported in several studies [10-13] but in our investigation the prepared TiO<sub>2</sub> nanopowder contains both anatase and rutile phase after annealing at  $800^\circ\text{C}$ .

Fig. 2 shows surface morphology of TiO<sub>2</sub> specimens annealed at temperatures  $600^\circ\text{C}$ - $800^\circ\text{C}$

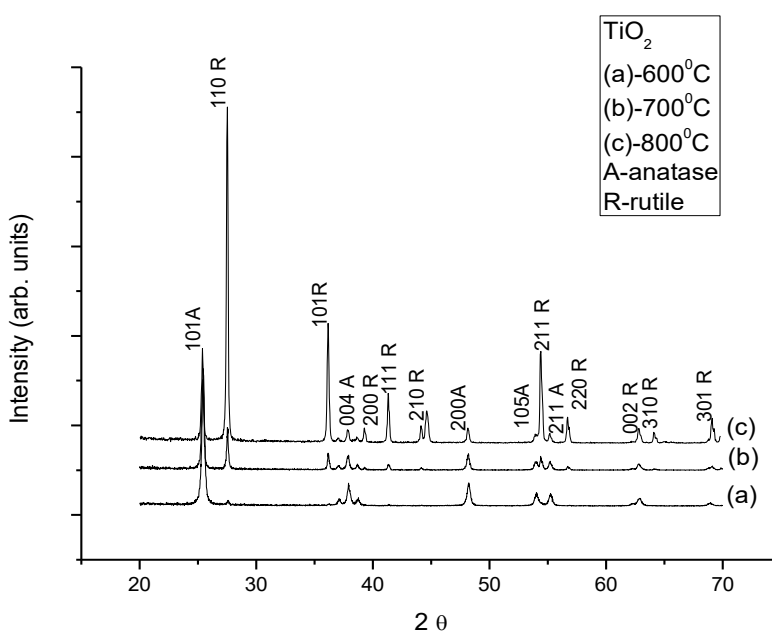


Fig.1. X-ray diffraction pattern of annealed TiO<sub>2</sub> nanopowder specimens.

Table 1. The average crystallite size, content of anatase and rutile phase and energy band gap values for TiO<sub>2</sub> specimens annealed at different temperatures.

Annealing temperature	Intensity I <sub>a</sub> (101 anatase)	Intensity I <sub>r</sub> (110 rutile)	Average crystallite size (nm)	Anatase %	Rutile %	Energy band gap (eV)
600°C	1456.56	32.55	35±5	97.26	2.74	2.93
700°C	976.44	446.93	45±5	63.37	36.62	2.75
800°C	943.63	3694.78	55±5	16.85	83.15	2.68

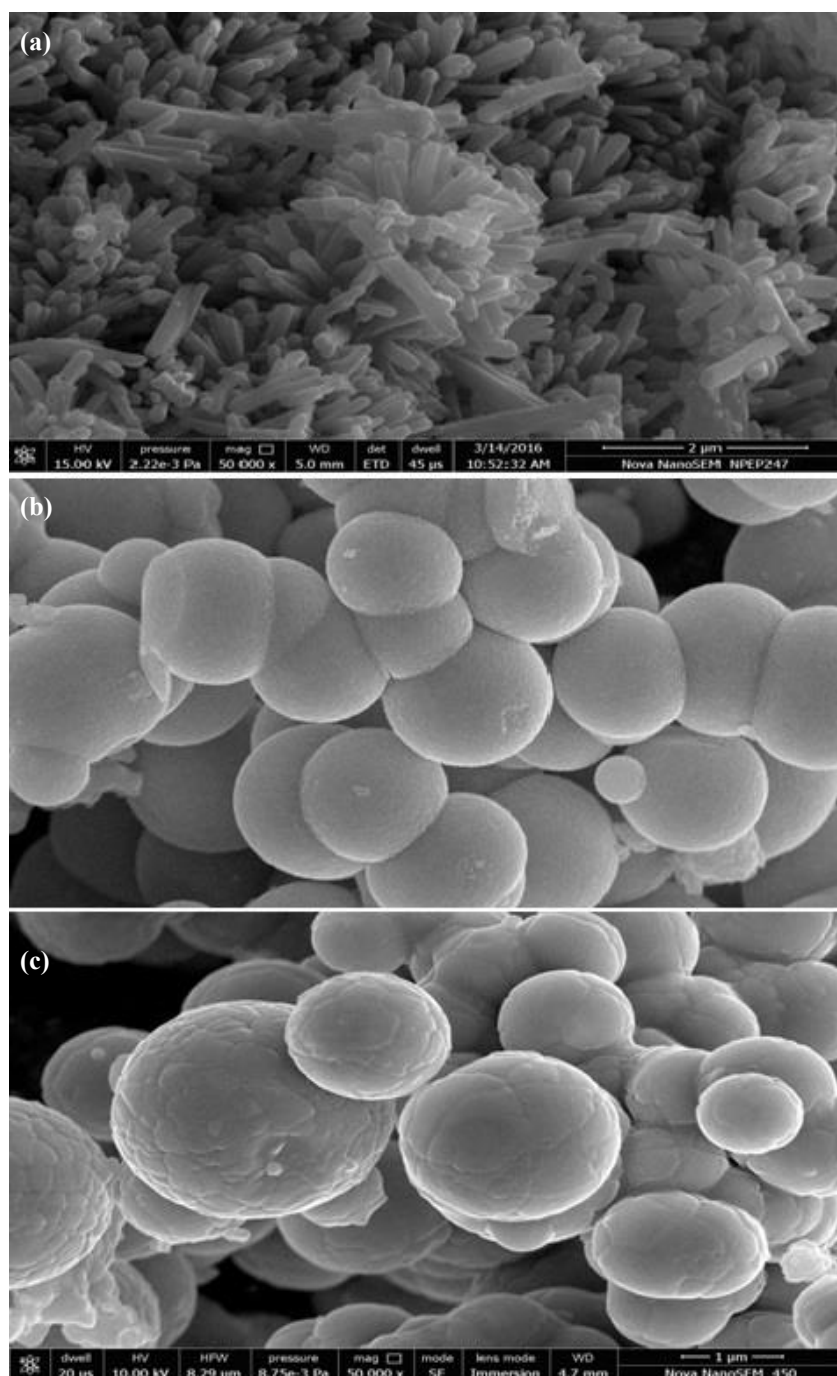


Fig. 2. SEM images of TiO<sub>2</sub> specimens annealed at (a) 600 °C (b) 700 °C and (c) 800 °C.

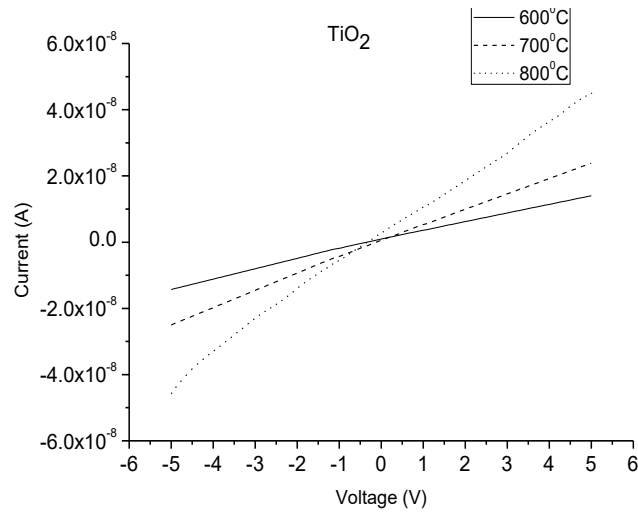


Fig. 3. I-V curves of TiO<sub>2</sub> specimens annealed at (a) 600 °C (b) 700 °C and (c) 800 °C.

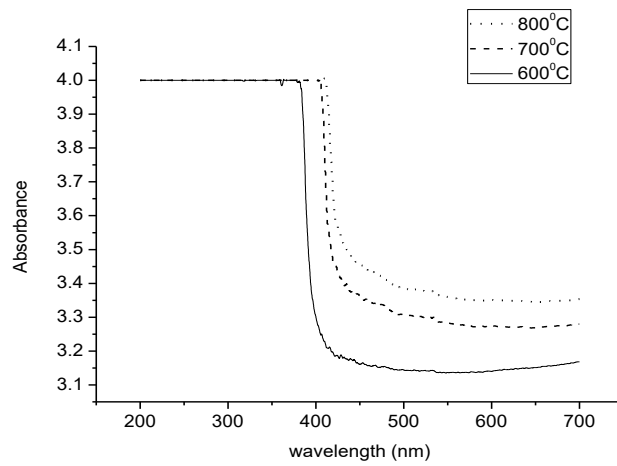
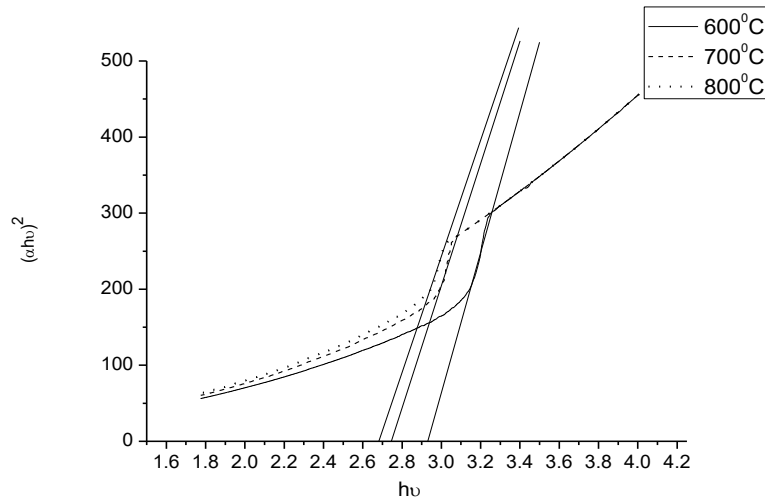


Fig. 4. (a) UV absorption spectra and (b) Tauc plot for TiO<sub>2</sub> specimens annealed at 600 °C, 700 °C and 800 °C.

°C using scanning electron microscopy (SEM). SEM image of TiO<sub>2</sub> specimen annealed at 600 °C show cylindrical shaped particles (Fig. 2 a) whereas SEM images of TiO<sub>2</sub> specimens annealed at 700°C and 800 °C show particles in spherical shape (Fig. 2 b and Fig. 2 c) [2, 14]. Fig. 3 depicts linear I-V curves of TiO<sub>2</sub> nanopowder specimens which confirm ohmic nature [15]. It is observed that current increases with increase in annealing temperature. This is due to the fact that an increase in crystallite size leads to improvement in electron migration. Therefore annealing of the TiO<sub>2</sub> nanopowder specimens increases average crystallite size which promises improved electrical properties [16].

UV-absorption spectra and Tauc plot for TiO<sub>2</sub> specimens annealed at different temperatures are shown in Fig. 4 (a) and Fig. 4 (b). The energy band gap values are obtained by extrapolating linear region to abscissa as shown in Fig. 4 (b) and are mentioned in Table 1. UV studies show that energy band gap increases with decrease in average crystallite size of TiO<sub>2</sub> nanopowder specimens corresponding to blue shift of the optical absorption edge [1, 17]. It is also observed that (see Table 1) energy band gap decreases with increase in annealing temperature. This is due to the fact that an increase in annealing temperature lowers of interatomic spacing [18-20]. It is noteworthy here that values of energy band gap obtained are lower as compared to energy band gap 3.2 eV for pure anatase , 3.0 for pure rutile phase and the data reported for the mixed phase TiO<sub>2</sub> nanopowder exhibiting as a capable candidate for gas sensing application [6, 7, 21].

## CONCLUSIONS

1. TiO<sub>2</sub> nanopowder exhibits lower energy band gap value which promises it as a suitable material for gas sensing application.
2. TiO<sub>2</sub> nanopowder contains both anatase and rutile phase after annealing in the temperature range 600 °C to 800 °C.

## ACKNOWLEDGMENTS

Authors thank Science & Engineering Research Board (SERB) for providing financial grant vide no SERB/F/5303/2014-15 and MRC, MNIT, Jaipur for providing XRD and SEM facilities.

## CONFLICT OF INTEREST

The authors declare that there is no conflict of interests regarding the publication of this manuscript.

## REFERENCES

1. Dai S, Wu Y, Sakai T, Du Z, Sakai H, Abe M. Preparation of Highly Crystalline TiO<sub>2</sub> Nanostructures by Acid-assisted Hydrothermal Treatment of Hexagonal-structured Nanocrystalline Titania/cetyltrimethylammonium Bromide Nanoskeleton. *Nanoscale Res Lett*, 2010; 5: 1829-1835.
2. Weiwei C, Hui Y, Xingzhong G. A Facile Synthesis of Nanocrystalline Spherical TiO<sub>2</sub> Particles and its Photoluminescent Properties. *Procedia Eng*, 2014; 94: 71-75.
3. Diebold U. The Surface Science of Titanium Dioxide. *Surf Sci Rep*, 2003; 48: 53-229.
4. Hanaor D A H, Sorrell C C. Review of the Anatase to Rutile Phase Transformation. *J Mater Sci*, 2011; 46: 855-874.
5. Enachi M, Lupan O, Braniste T, Sarua A, Chow L, Mishra Y K, Gedamu D, Adelung R, Tiginyanu I. Integration of Individual TiO<sub>2</sub> Nanotube on the Chip: Nanodevice for Hydrogen Sensing. *Phys Status Solidi RRL*, 2015; 9: 171-174.
6. Pawar S, Chougule M, Patil S, Raut B, Dalvi D, Patil P, Sen S, Joshi P, Patil V. Fabrication of Nanocrystalline TiO<sub>2</sub> Thin Film Ammonia Vapor Sensor, *J Sens Technol*, 2011; 1: 9-16.
7. Pawar S G, Chougule M A, Godse P R, Jundale D M, Pawar S A, Raut B T, Patil V B. Effect of Annealing on Structure, Morphology, Electrical and Optical Properties of Nanocrystalline TiO<sub>2</sub> Thin Films. *J Nano Electron Phys*, 2011; 3: 185-192.
8. Zhu T, Ong W L, Zhu L, Ho G W. TiO<sub>2</sub> Fibers Supported  $\beta$ -FeOOH Nanostructures as Efficient Visible Light Photocatalyst and Room Temperature Sensor. *Sci Rep*, 2015; 5:10601 doi:10.1038/srep10601.
9. Vijayalakshmi K, Rajendran V. Synthesis and Characterization of Nano-TiO<sub>2</sub> via Different Methods. *Arch Appl Sci Res*, 2012; 4: 1183-1190.
10. Chaudhary V, Srivastava A, Kumar J. On the Sol-gel Synthesis and Characterization of Titanium Oxide Nanoparticles, *Mater Res Soc Symp Proc*, 2011; 1352: doi: 10.1557/opl.2011.759.
11. Cesnovar A, Paunovic P, Grozdanov A, Fidanchevska E. Preparation of Nano-crystalline TiO<sub>2</sub> by Sol Gel Method Using Titanium Tetraisopropoxide (TTIP). *Adv Nat Sci: Theory Appl*, 2012; 1:133-142.
12. Hanaor D A H, Chironi I, Karatchevtseva I, Triani G, Sorrell C C. Single- and Mixed-Phase TiO<sub>2</sub> Powders Prepared by Excess-Hydrolysis of a Titanium Alkoxide. *Adv Appl Ceram*, 2012; 111: 149-158.
13. Mehranpour H, Askari M, Ghamsar M Sasani, Farzalibeik H. Study on the Phase Transformation Kinetics of Sol-gel Derived TiO<sub>2</sub> Nanoparticles. *J Nanomater*, 2010;doi:10.1155/2010/626978
14. Bakardjieva S, Subrt J, Stengl V, Dianež M J, Sayagues M J. Photoactivity of Anatase–Rutile TiO<sub>2</sub> Nanocrystalline Mixtures Obtained by Heat Treatment of Homogeneously Precipitated Anatase. *Appl Catal B*, 2005; 58: 193-202.
15. Prasad A K, Dhonge B P, Mathews T, Dash S, Shwathya R, Tyagi A K, Murali N. Microstructure Dependent Ammonia Sensing Properties of Nanostructured Zinc Oxide Thin Films Using in-House Designed Gas Exposure Facility. *Nanoscience, Engineering and Technology (ICONSET) IEEE*, 2011; 978: 73-77.
16. Ahmad M K, Rasheid N A, Ahmed A Z, Abdullah S, Rusop M. Effect of Annealing Temperature on Titanium Dioxide Thin Films Prepared by Sol Gel Method. *J Fiz Mal*, 2008;

- 29: 71-74.
17. Tripathi A K, Singh M K, Mathpal M C, Mishra S K, Agarwal A. Study of Structural Transformation in TiO<sub>2</sub> Nanoparticles and Its Optical Properties. *J Alloys Compd*, 2013; 549: 114-120.
18. Zareen A, Ali S, Irfan M. The Effect of Annealing Temperatures on Phase and Optical Properties of TiO<sub>2</sub> Nanoparticles for Solar Cell Applications. *ESJ*, 2014; 2: 447-450.
19. Yoo D, Kim I, Kim S, Hahn C H, Lee C, Cho S. Effects of Annealing Temperature and Method on Structural and Optical Properties of TiO<sub>2</sub> Films Prepared by RF Magnetron Sputtering at Room Temperature. *Appl Surf Sci*, 2007; 253: 3888-3892.
20. Vasantkumar C V R, Mansingh A. Structural Evolution and Optical Properties of TiO<sub>2</sub> Thin Films Prepared by Thermal Oxidation of Sputtered Ti Films. *Seventh IEEE International Symposium on Application of Ferroelectrics*, IEEE, New York, 1990; 713-716.
21. Li Z, Ding D, Liu Q, Ning C. Hydrogen Sensing with Ni-Doped TiO<sub>2</sub> Nanotubes. *Sensors*, 2013; 13: 8393-8402.